Original Article

Institution of MECHANICAL ENGINEERS
Journal of POWER AND ENERGY

Proc IMechE Part A:
J Power and Energy
2015, Vol. 229(6) 677–688

DOI: 10.1177/0957650915587433
pia.sagepub.com
SAGE

Energy and economic analysis of concentrating solar power plants based on parabolic trough and linear Fresnel collectors

Daniele Cocco and Giorgio Cau

Abstract

This paper compares the performance of 1 MWe concentrating solar power (CSP) plants based on an organic Rankine cycle (ORC) power generation unit integrated with parabolic trough and linear Fresnel collectors. The CSP plants studied herein use thermal oil as heat transfer fluid and as storage medium in a two-tank direct thermal storage system. The performance of the CSP plants was evaluated on the basis of a 1 MWe ORC unit with a conversion efficiency of about 24%. The comparative performance analysis of the two CSP solutions was carried out by means of specifically developed simulation models and considering different values of solar multiple and thermal storage capacity. The results of the performance assessment demonstrate that CSP plants based on linear Fresnel collectors lead to higher values of electrical energy production per unit area of occupied land (about 50–60 kWh/y per m^2 vs. 45–55 kWh/y m^2 produced by solutions based on parabolic troughs). However, owing to their better optical efficiency, the use of parabolic troughs gives better values of energy production per unit area of solar collector (about 185–205 kWh/m^2 vs. 125–140 kWh/m^2) and, therefore, better conversion efficiencies (about 10.8–11.9% vs. 7.3–8.1%). The results of a preliminary economic analysis show that CSP plants based on linear Fresnel collectors are still not competitive with those based on parabolic trough owing to their higher energy production cost (about 380 €/MWh vs. 340 €/MWh).

Keywords

Concentrating solar power plants, parabolic trough collectors, linear Fresnel collector

Date received: 9 July 2014; accepted: 24 April 2015

Introduction

The goal of reducing fossil fuel consumption and the related CO_2 emissions can be achieved only by a strong development of renewable energy technologies. Among the different renewable energy sources (RES), solar energy is the most abundant one and can greatly contribute to achieving the previously mentioned goal. Energy production from photovoltaic (PV) systems has greatly increased in recent years and the overall installed PV capacity in the world is around 100 GW (over 28 GW of additional power was installed in 2012).[1]

In the field of solar energy conversion technologies, the most interesting alternative to PV systems is represented by concentrating solar power (CSP) plants. In CSP plants, concentrating solar collectors are used to increase the temperature of a heat transfer fluid (HTF) and, therefore, to produce high temperature thermal energy, which is subsequently converted into mechanical work by a suitable power generation section. CSP plants are usually coupled with a thermal energy storage (TES) system to offset the intermittence of solar energy and increase power plant dispatchability. Today the current CSP world generating capacity is around 4100 MW and is rapidly increasing. More than 1700 MW of additional capacity are currently under construction and an installed CSP capacity of about 15 GW is expected before 2020. Spain is the country with the highest CSP production, thanks to the operation of more than 40 power plants with an installed capacity of more than 2 GW.[2,3]

With reference to CSP plants, different options are available for solar field (parabolic trough, linear Fresnel, solar tower and solar dish systems), power block (steam Rankine and organic Rankine cycles, Stirling engines, combined cycles, etc.), heat transfer

Department of Mechanical, Chemical and Materials Engineering, University of Cagliari, Cagliari, Italy

Corresponding author:
Daniele Cocco, Department of Mechanical, Chemical and Materials Engineering, University of Cagliari, Via Marengo, 2 - 09123 Cagliari, Italy.
Email: daniele.cocco@unica.it

fluid (thermal oil, molten salts, steam, etc.), and thermal energy storage section (active, passive, two-tank, thermocline, etc.).[4–7]

As a general rule, the construction of large-size power generation units (more than 20–30 MW) is today the preferred choice due to the best trade-off between capital costs and overall conversion efficiency. Most CSP plants use parabolic trough collectors (PTC), thermal oil as HTF and molten salts as heat storage medium. The power generation section is almost always based on steam Rankine cycles with superheated steam produced at about 370–380 °C and 80–100 bar, high-pressure and low-pressure steam turbines with reheating and 4–6 steam extractions for feed-water heating. Most of the 50 MWe Spanish CSP units are based on this configuration.[2,3]

To improve the performance of CSP plants and reduce their energy production costs, one of the main R&D activities aims to raise the maximum temperature of the HTF by using molten salts or the direct production of steam.[8–12] Other interesting solutions for large-size CSP plants rely on solar tower systems[13,14] and hybrid systems where the solar field is integrated with a conventional fossil fuel power plant.[15–17]

As mentioned, large-size CSP plants give the best trade-off between conversion efficiency and capital costs but it should also be observed that the construction of a commercial 50 MWe unit requires a total capital investment of about 250–300 M€ and the availability of about 150–250 hectares of land. However, in countries where the wide extension areas required by large-size CSP plants can be hard to find, medium-size CSP plants (around 1 MWe) may be a more suitable option due to the lower land requirement. Moreover, medium-size power plants require lower capital investments and are also a very interesting solution for the diffusion of distributed power generation.

The most suitable technology options for the solar field and power block of medium-size CSP plants differ from those of large-size plants. In fact, steam turbines are generally not suitable for power outputs in the range of 1 MWe and, therefore, the power generation section of such CSP plants cannot be based on steam Rankine cycles. One of the most interesting alternatives is represented by organic Rankine cycles (ORC), where steam is substituted by organic fluids with high molar weight. Such ORC systems require thermal energy inputs with temperature levels in the range of 250–350 °C and give conversion efficiencies of about 20–25%.[18–20] Moreover, with such temperature levels, linear concentrating collectors appear to be the most suitable option and linear Fresnel collectors (LFC) may be a viable alternative to PTC, especially if the land requirement is a key feature. In comparison to PTC, LFCs have a simpler design, use less expensive mirrors and tracking systems, show lower land requirements and lower capital costs. On the other hand, the optical efficiency of LFC is lower than that of PTC.[21–24] Finally, for medium-size CSP units working with thermal oil the most suitable option for the TES section is based on a two-tank direct system using thermal oil as heat transfer fluid and storage medium.[6,25,26]

To explore the capabilities of medium-size units, this paper reports a comparative performance and economic analysis of CSP plants using PTCs and LFCs, thermal oil as heat transfer fluid and an ORC power generation unit. The CSP plants studied herein also include a two-tank direct thermal storage system based on the use of the same thermal oil as storage medium. The comparative study was carried out on the basis of a 1 MWe ORC plant by considering different values for both the solar multiple and thermal storage capacity. In particular, the study aims to evaluate the expected annual energy production of the two CSP options with reference to the collecting and land area requirement. Moreover, a preliminary assessment of the energy production cost was also carried out.

CSP power plant configuration

Figure 1 shows a simplified diagram of the CSP plant considered in this paper. The CSP plant includes three main sections: the solar field, the power block and the thermal energy storage system.

The solar field is based on several rows of parabolic trough or LFCs connected in parallel to achieve the required thermal oil mass flow and therefore the required thermal power output. PTC and LFC are designed for the same thermal power output and the same input and outlet thermal oil temperatures. However, due to the different geometrical structure and collector efficiency, the collecting area and the required number of rows show a significant variation.

For both PTC and LFC, each collector row includes several collector modules connected in series. The solar collector rows are aligned along the North-South direction and are equipped with a single-axis tracking system that allows to follow the sun path from East to West. Overall, LFCs are less expensive than PTCs, using flat mirrors (or mirrors with only a very small curvature), a lighter supporting structure and a simpler tracking system. However, the optical efficiency of LFCs is lower than that of PTCs.

As shown in Figure 1, the power block is based on an ORC unit, where thermal energy is converted to electrical energy by using an organic fluid (a siliconic oil in this case) that follows a regenerated Rankine cycle. The condensing heat of the ORC unit is removed by a cooling tower. Moreover, the TES section of the CSP plant studied here is based on a two-tank direct system using the same thermal oil as the storage medium.

The piping system of the CSP plant includes the two circulating thermal oil pumps, the cold and hot header pipe (one for distributing the cold oil

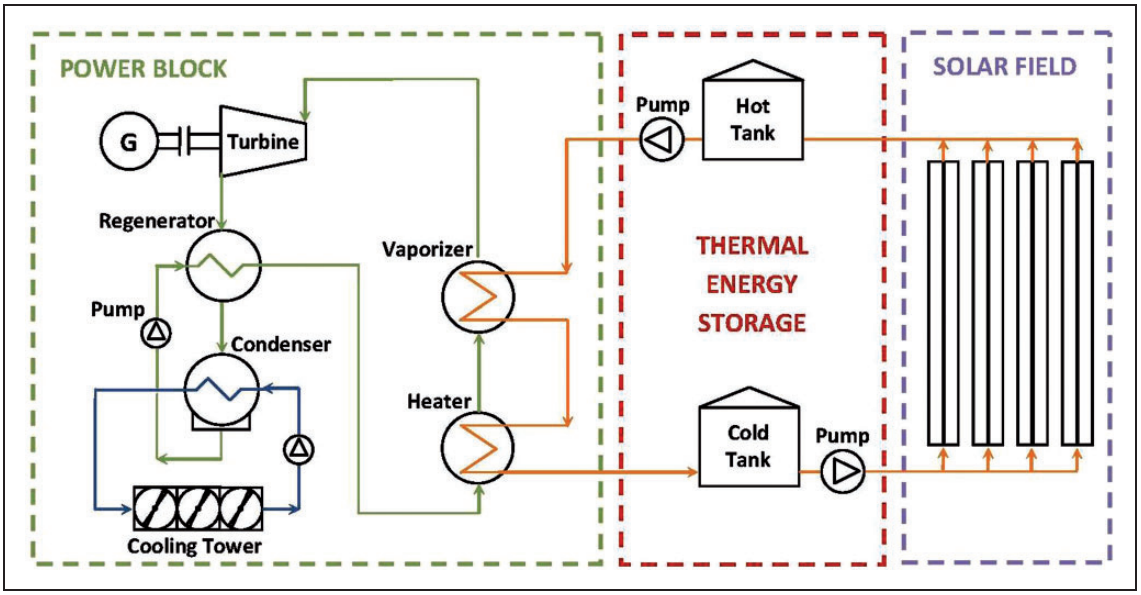

Figure 1. Process flow diagram of the CSP power plant.

throughout the collector loops and the other for collecting the hot oil), the main pipes, valves, fittings and pressure, temperature and flow meters.

System modeling and assumptions

The performance of the CSP plants was evaluated on a yearly basis by means of a specifically developed simulation model. In particular, the simulation model evaluates the performance of PTC and LFC as a function of solar radiation and solar position for given values of the main geometrical and technical characteristics of solar collectors, as well as for assigned thermodynamic properties of the heat transfer fluid.

The solar energy available for a CSP plant is conventionally defined by the product of direct normal irradiation (DNI) and collecting area A_C. For PTC the collecting area is represented by the aperture area of the parabola, while for LFC it is given by the overall area of the mirror rows. Evaluation of the annual energy production of CSP plants requires the availability of detailed data (at least on an hourly basis) about solar radiation and solar position.

The present comparative study was carried out by using a data set for a typical meteorological year obtained from the Meteonorm software[27] for the site of Cagliari (39°13'25"N, 9°07'20"E), in the south of Sardinia (Italy). In particular, the meteorological data set includes DNI, solar azimuth and elevation, ambient temperature (dry and wet bulb), relative humidity and wind velocity. Figure 2 gives the frequency distribution of the DNI for the site of Cagliari and Table 1 summarizes the most important meteorological data and the design conditions assumed for the comparative analysis. In particular, the design conditions refer to the average meteorological data at noon on 21 June.

For a given collector geometry, the incidence angle depends on the solar position, which is completely defined by the azimuth angle γ (that is, the angle between the projection of the solar rays on the horizontal plane and the south direction) and the elevation angle α (that is, the angle between solar rays and their projection on the horizontal plane). Moreover, two different components of the incidence angle θ are calculated: the longitudinal component θ_L (the angle between the direction normal to the horizontal surface and the projection of the solar rays on the longitudinal plane of the collector) and the transversal component θ_T (the angle between solar rays and their projection on the transversal plane of the collector). These two components can be expressed in function of γ and α by means of the following equations

$$\tan(\theta_T) = \frac{\sin(\gamma)}{\tan(\alpha)} \quad (1)$$

$$\sin(\theta_L) = \cos(\gamma) \cdot \cos(\alpha) \quad (2)$$

It should be observed that in the case of PTC, the tracking system allows rotation of the overall collector along its longitudinal axis such that the vector normal to the collector aperture area is always contained in the same plane as the solar rays. Therefore, the component θ_T directly gives the rotation angle of the PTC during the daily sun path.

The simulation model used in this comparative study evaluates the thermal power output and the conversion efficiency of the overall solar field as a function of solar radiation and solar position. The simulation model is mainly based on the energy balance of the solar collector, which includes two main components: the solar concentrator and the receiver

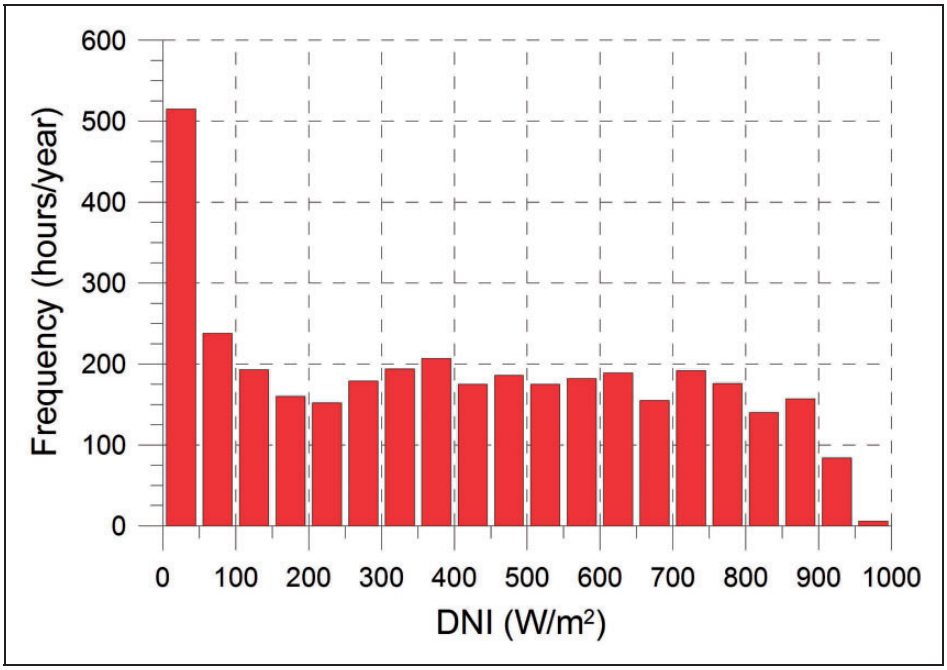

Figure 2. Frequency distribution of the DNI for the site of Cagliari.

Table 1. Meteorological data for the site of Cagliari.

Available DNI	1720 kWh/m^{2}y
Average ambient temperature	17.2°C
Average wind velocity	3.96 m/s
Design DNI	800 W/m^2
Design elevation/azimuth angles	74.2°/0.0°
Design dry/wet bulb temperatures	32.0/22.0°C

DNI: direct normal irradiation.

tube. The energy balance of the solar concentrator gives

$$Q_{SOL} = A_C \cdot DNI = Q_{RCV} + Q_{OPT} \tag{3}$$

In equation (3), Q_{SOL} denotes the solar power input (i.e. the available direct solar radiation), Q_{RCV} is the thermal power concentrated on the receiver tube, and Q_{OPT} are the optical losses of the solar concentrator. In particular, thermal power Q_{RCV} has been evaluated here by means of the following equation

$$Q_{RCV} = A_C \cdot DNI \cdot \eta_{OPT,R} \cdot IAM(\theta) \cdot \eta_{END} \cdot \eta_{SHD} \cdot \eta_{CLN} \tag{4}$$

As shown by equation (4), the thermal power available for the receiver tube is lower than the solar power input owing to the presence of different types of optical losses. Reference optical efficiency $\eta_{OPT,R}$ depends on mirror reflectivity, glass tube transmissivity, absorptivity of the selective coating of the receiver tube, imperfections in the collector mirrors, tracking errors, shading of receiver supports on mirrors, etc. Reference optical efficiency is commonly evaluated for $\theta = 0^\circ$ because the optical properties of the different materials (mirrors, glass tube, selective coating) and the relative shading depend on the incidence angle of the incoming solar rays. For this reason, reference optical efficiency is multiplied by the incidence angle modifier (IAM) to give the effective optical efficiency. The IAM depends on the incidence angle θ and is often divided into the longitudinal and transversal IAM components:

$$IAM(\theta) = IAM(\theta_L) \cdot IAM(\theta_T) \tag{5}$$

Figure 3 shows the two IAM components considered in this study for linear Fresnel and parabolic trough collectors in function of the longitudinal and transversal components θ_L and θ_T.[23,28] It should be noted that for PTC the IAM transversal component can always be assumed equal to 1 because the vector normal to the collector aperture is always contained in the same plane as the solar rays.

With longitudinal components θ_L higher than 0°, the useful mirror area of linear collectors is reduced by the geometrical end-losses, which depend on collector length L and focal length F. Overall, these losses are taken into account by means of the end-loss optical efficiency

$$\eta_{END} = 1 - \frac{F}{L} \cdot \tan\theta_L \tag{6}$$

Moreover, in equation (4), the term η_{CLN} is mirror and glass tube surface cleanliness efficiency and η_{SHD} is the shadow efficiency, which gives the

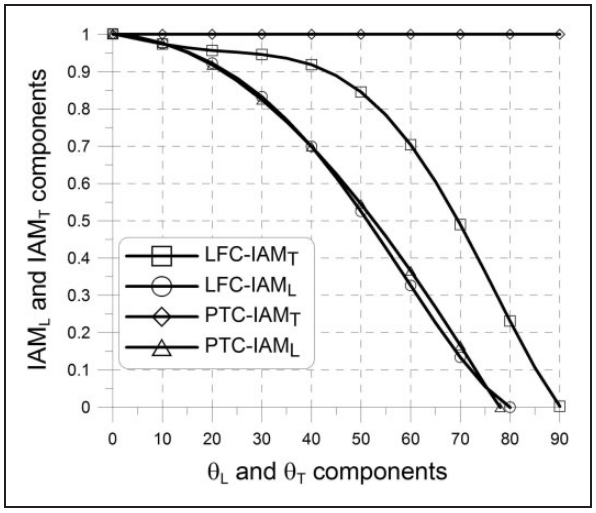

Figure 3. Longitudinal and transversal IAM components.

energy losses due to the shadow from the different rows of collectors. Shadow efficiency applies only to solar fields with multiple rows of PTC and is given by the following equation

$$\eta_{SHD} = 1 - \frac{R}{W} \cdot \tan\theta_T \tag{7}$$

where R is the distance between the PTC rows and W the collector aperture width.

Thermal power Q_{FLD} transferred to the thermal oil is given by the difference of receiver available power Q_{RCV} and thermal losses of solar field Q_{THR}

$$Q_{FLD} = m_O \cdot Cp_O \cdot \left(T_{O,out} - T_{O,in}\right) = Q_{RCV} - Q_{THR} \tag{8}$$

Thermal losses were evaluated by the sum of receiver thermal losses and piping thermal losses

$$\begin{aligned} Q_{THR} &= \left[q_{tube} + q_{pipe}\right] \cdot A_C \\ &= \left[\left(a_1 \cdot T + a_2 \cdot T^2\right) + q_{pipe}\right] \cdot A_C \end{aligned} \tag{9}$$

where ΔT is the difference between average oil temperature in the receiver tube and ambient temperature.

Table 2 shows the main geometrical and performance parameters of PTC and LFC used in the following comparative study.[4–7,21–24] The main power consumption of the solar field is due to the collector tracking system and the oil circulating pumps. The first term was assumed equal to 1.5 W/m^2 of collecting area. The design conditions of piping and oil pumps were evaluated by imposing a fluid velocity of about 1 m/s and a pump efficiency equal to 75%. The power required by oil pumps during the daily operation depends on the square of the oil mass flow.

Table 2. Main geometrical and performance parameters of PTC and LFC.

	PTC	LFC
Collector length L	150 m	150 m
Collector width W	5.77 m	16.56 m
Collector area A_C	865.5 m^2	1712.0 m^2
Focal length F	1.71 m	7.40 m
Lines distance R	17.31 m	4.00 m
Reference optical efficiency $\eta_{OPT,R}$	0.75	0.67
Cleanliness efficiency η_{CLN}	0.98	0.98
Inlet/outlet oil temperature	204°C/305°C	204°C/305°C
a_1 coefficient	–	0.056 W/m^{2}K
a_2 coefficient	0.00047 W/m^{2}K^2	0.000213 W/m^{2}K^2
Specific piping losses q_{pipe}	5 W/m^2	5 W/m^2

PTC: parabolic trough collector; LFC: linear Fresnel collector.

Table 3. Operating parameters of the ORC unit.

Gross power output	1000 kW
Thermal power input	4043 kW
Oil inlet/outlet temperature	305°C/204°C
Condenser power output	3040 kW
Water inlet/outlet temperature	25°C/35°C
Gross electrical efficiency	24.7%
ORC internal consumption	3.6% of gross power
Cooling tower electrical consumption	0.6% of cond. power

ORC: organic Rankine cycle.

In particular, for this comparative analysis, the power consumption of the oil pumps is 32 W/(kg/s)^2.

The power block considered in this comparative performance analysis is an ORC unit with a power output of 1 MWe integrated with a closed circuit cooling tower. Design and off-design performance of the ORC module were evaluated with reference to data available for commercial units.[29] In particular, Table 3 reports the most important operating parameters of the ORC unit while Figure 4 shows its off-design efficiency as a function of thermal load (cooling water at 25 °C) and wet bulb temperature (thermal power input of 4043 kW and 3 °C of temperature difference between cooling water and wet bulb temperature).

As already mentioned, the TES system considered here is based on a direct system using two identical thermal oil tanks. The mass and volume of thermal oil to be stored were evaluated in function of the required storage capacity (here expressed in terms of equivalent hours of ORC thermal supply) and thermodynamic properties of thermal oil (for the design of the two

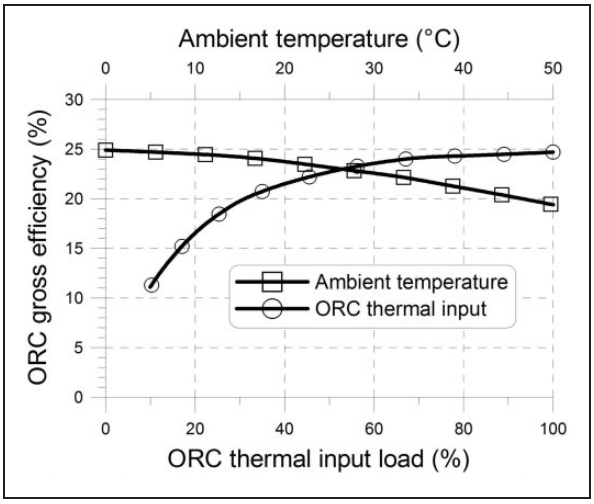

Figure 4. Off-design efficiency of the ORC unit.

storage tanks, an average specific heat of 2.5 kJ/kgK and a density of 750 kg/m^3 at 305 °C were assumed here). Moreover, the volume of each storage tank was increased by 10% compared to the thermal oil volume. Finally, a thermal energy loss of 2% of stored energy was considered.

Performance of CSP plants

For a given power output of the ORC unit, the extension of the solar field and the capacity of the TES section mainly depend on two important design parameters: the solar multiple (SM) and storage capacity (SC). The solar multiple is the ratio between the thermal power produced by the solar field at design conditions and the thermal power required by the power block at nominal conditions and therefore increasing the solar multiple increases the thermal power output of the solar field. CSP plants are usually designed for SM values higher than one to increase the thermal power output of the solar field even during periods with DNI lower than the design one and operate the power block at nominal conditions for longer periods of time. In particular, SM values higher than 1.5–2.0 are usually adopted in CSP plants integrated with a TES section. Obviously, increasing the solar multiple increases the collecting area of the solar field and therefore the land area required by the CSP plant. Land area depends on number, width and distance of the collector rows, the free space around the collectors (10 m in this case) and the area required by the power block and the TES section (here assumed equal to 2500 m^2). Figure 5 shows the collecting area and the land requirement for CSP plants based on PTC and LFC in function of SM (plot labels also give the corresponding number of collector rows and the thermal power output of the solar field at design conditions).

As shown in Figure 5, for a given solar multiple (and therefore for a given thermal power output of the solar field), CSP plants based on LFC require a larger collecting area (by about 12–13%) than PTC due to lower conversion efficiency of the solar field (which is given by the ratio of thermal power Q_{FLD} transferred to the thermal oil and solar power input Q_{SOL}). It should be noted that the latter conversion efficiencies are lower than the optical reference value of Table 3 even at design conditions due to the thermal and optical losses previously discussed (shadowing, end losses, IAM, etc.). In particular, at design conditions the efficiency of the PTC solar field is around 67.3% while that of the LFC one is about 59.5%. The bottom part of Figure 5 also demonstrates that the CSP-LFC solution requires a lower collecting area and about 50% less land area than the CSP-PTC plant due to higher collector width and the shorter distance between the rows (4.0 m instead of 17.31 m).

The Storage Capacity (SC) of a CSP plant is usually expressed in terms of equivalent hours of thermal supply of the power block. Therefore, the volume of each storage tank and the mass of thermal oil contained therein depends only on SC because the product of ORC thermal power input and the equivalent hours of storage capacity directly gives the energy to be stored by the TES section. In particular, for the ORC considered here (4043 kW of required thermal power input), 1 hour of storage capacity requires two storage tanks with a volume of about 85 m^3 (6 m diameter and 3 m high, for example) and 58 t of thermal oil. Obviously, tank volume and mass of thermal oil linearly increase with the TES storage capacity.

Figure 6 shows the net electrical production on a yearly basis for the two CSP configurations in function of both solar multiple (SM) and equivalent hours of thermal energy storage (SC). For both CSP solutions, annual energy production increases with SM and SC even though the increase in storage capacity improves net energy production only for increasing values of SM. For given values of both SM and SC, the CSP-PTC solution gives higher energy yields in comparison to the CSP-LFC one owing to its better solar field efficiency.

As mentioned, in many countries (and in Italy in particular) the finding of large areas required by CSP plants can be difficult and therefore an important performance parameter of such power plants is specific energy production per unit area of solar field. For this reason, Figure 7 reports the specific annual energy production of the CSP configurations studied here in function of both SM and SC. In particular, the bottom part of Figure 7 refers to energy production per unit area of collector aperture while the upper part refers to energy production per unit area of required land.

Figure 7 demonstrates the importance of a proper trade-off between solar multiple and storage capacity to maximize the specific energy production. Moreover, Figure 7 demonstrates that if land availability is the most limiting factor, CSP solutions based

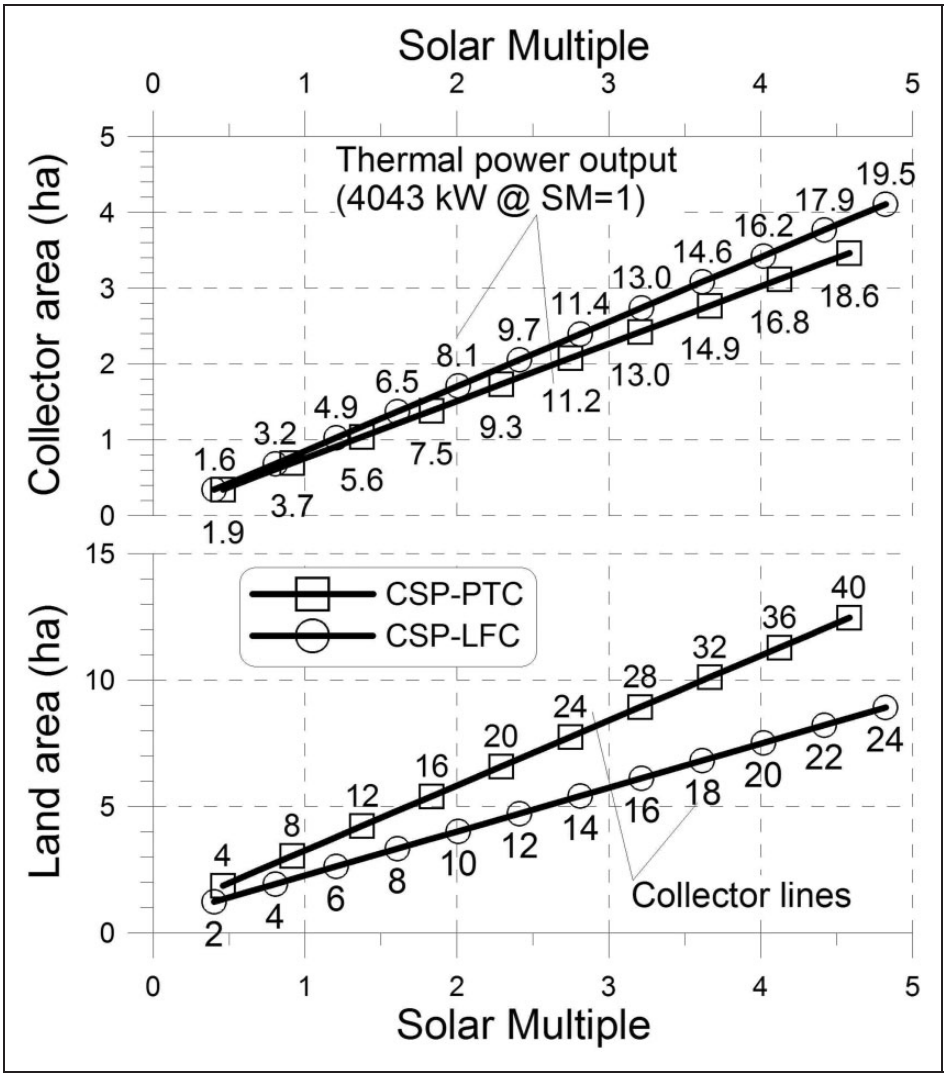

Figure 5. Collectors and land area for CSP plants in function of SM.

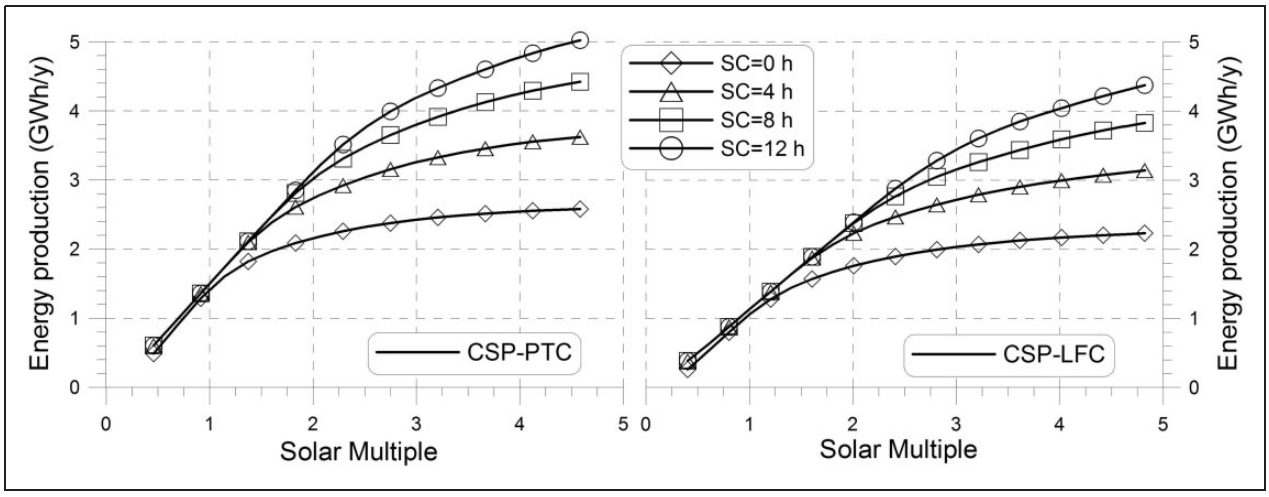

Figure 6. Annual energy production of the two CSP power plants in function of solar multiple and energy storage capacity.

on LFCs can be a very interesting option owing to their high energy production per m^2 of occupied land. In the field of storage capacities considered here, for CSP-LFC plants the highest specific production per m^2 of occupied land is about 50–60 kWh/y. In particular, without any thermal energy storage (SC = 0) the highest specific production of the CSP-LFC solution is about 49 kWh/y per m^2 of occupied land and is

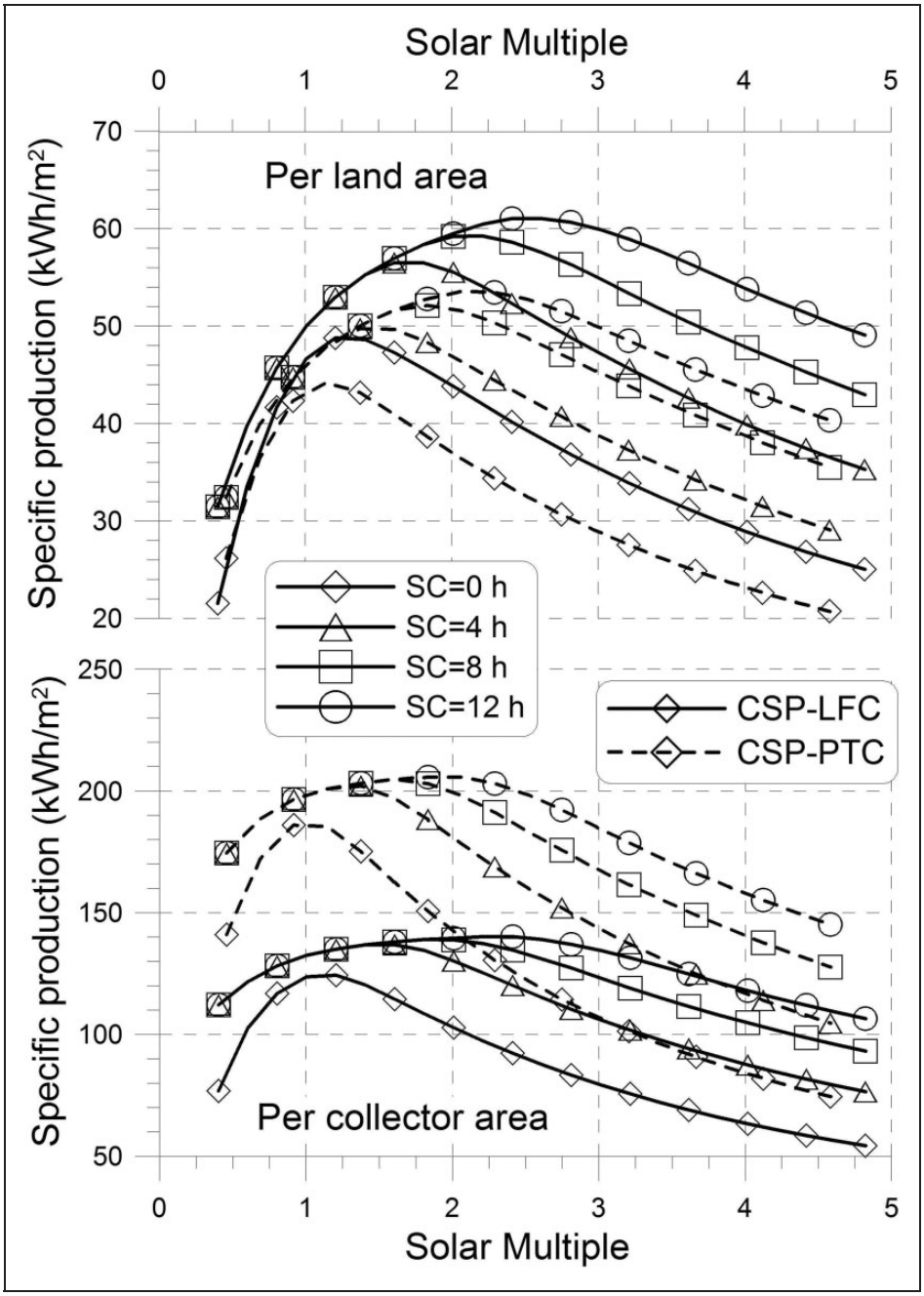

Figure 7. Specific energy production of the two CSP power plants in function of solar multiple and energy storage capacity.

achieved with a SM value around 1.2. As shown in Figure 7, the increase in SC increases the highest specific production and for SC = 12 h the highest specific production of the CSP-LFC solution is about 61 kWh/y per m^2 of occupied land and is achieved with a SM value around 2.5. Figure 7 shows that the highest specific production of CSP-PTC plants is about 45–55 kWh/y per m^2 of occupied land and that it is achieved with lower SM values (around 1.1 for SC = 0 and around 2.0 for SC = 12 h).

On the other hand, the bottom side of Figure 7 demonstrates that the CSP solutions based on PTC give higher values of specific energy production per unit area of collector aperture (about 185–205 kWh/m^2 vs. 125–140 kWh/m^2), owing to their better optical efficiency in comparison to the LFC solutions. Obviously, as annual solar energy available per m^2 of collector area is the same for all CSP solutions (1720 kWh/m^2y for the site of Cagliari), energy production per unit area of collector aperture is proportional to the average conversion efficiency of the CSP plant. For example, the aforementioned maximum values of the specific energy production of CSP-PTC plants (about 205 kWh/m^2 achieved for SC = 12 h and SM = 2.0) leads to an average conversion efficiency of about 11.9% while that of the CSP-LFC plant (140 kWh/m^2 achieved for SC = 12 h and SM = 2.2) gives an average efficiency of about 8.1%.

Table 4. Assumptions for the economic analysis of CSP systems.

	PTC	LFC
Solar field specific cost	275 €/m^2 of collector area	200 €/m^2 of collector area
ORC specific cost	1000 €/kWe of nominal power output	
TES specific cost	1250 €/m^3 of storage volume	
Thermal oil cost	2 €/kg	
Piping specific cost	30 €/m^2 of collector area	
Land cost	10 €/m^2	
Balance of plant cost	250 €/kWe of nominal power output	
Engineering cost	20% of purchase and BoP cost	
O&M annual cost	1.5% of total capital cost	
Annual interest rate	7%	
Operating lifetime	25 years	

PTC: parabolic trough collector; LFC: linear Fresnel collector; ORC: organic Rankine cycle; TES: thermal energy storage.

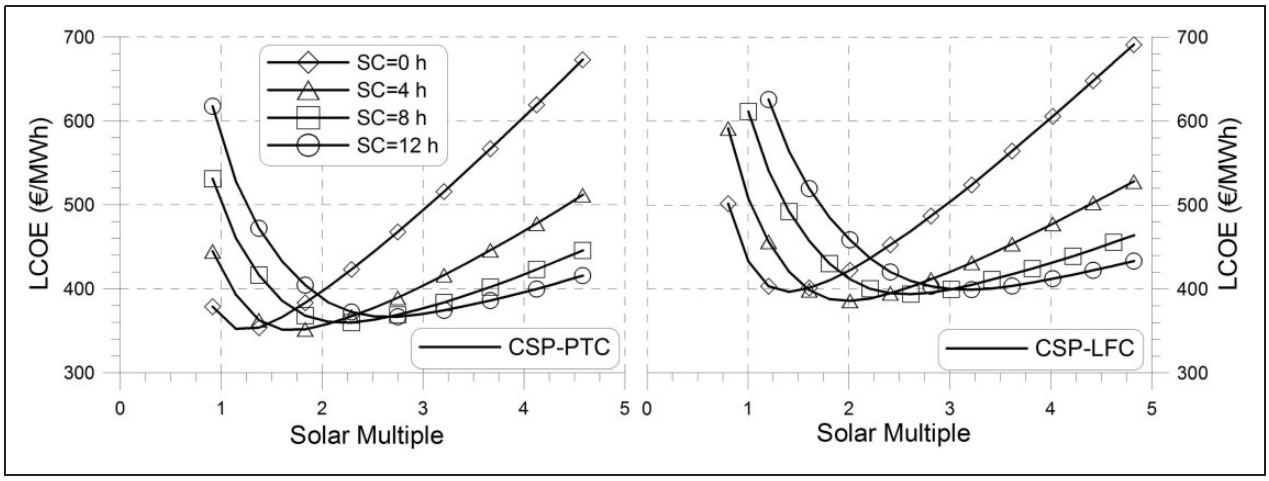

Figure 8. LCOE of the two CSP power plants in function of solar multiple and energy storage capacity.

Energy production cost

For a given power generation section, CSP systems based on PTC and LFC require different solar field extensions and therefore different capital costs. Moreover, these two CSP systems also give different annual energy productions and therefore show different energy production costs. For this reason, a preliminary economic analysis to evaluate the energy production cost of CSP-PTC and CSP-LFC plants was carried out in this paper.

In particular, the economic analysis calculates the levelized cost of electricity (LCOE) according to the simplified methodology proposed by the International Energy Agency (IEA).[30] The LCOE was calculated here by means of the following equation

$$\mathrm{LCOE} = \frac{\mathrm{TCI} + \sum_{k=1}^{N} \left(I_k + C_{O\,M,k}\right) \cdot (1+i)^{-k}}{\sum_{k=1}^{N} (E_k) \cdot (1+i)^{-k}} \qquad (10)$$

where TCI is the total capital investment, I_k are the additional investment cost in year "k", $C_{O\&M,k}$ are the operation and maintenance costs in year "k", E_k is the electricity production in year "k", i is the annual interest rate, and N the operating lifetime. For simplicity, TCI has been concentrated at the beginning of the operating lifetime and the investment cost in the following years has been neglected. Moreover, annual operation and maintenance costs and annual electricity production have been assumed herein as constant during the overall operating lifetime. Total capital investment was estimated on the basis of published information on purchased equipment costs of the main plant components and by adding the Balance of Plant and engineering costs.[21–26] Table 4 shows the main assumptions used for the economic analysis.

Figure 8 shows the LCOE of CSP systems in function of SM and SC. In particular, the left side of Figure 8 gives the LCOE of the CSP-PTC solution, while the right side gives the LCOE of the CSP-LFC one.

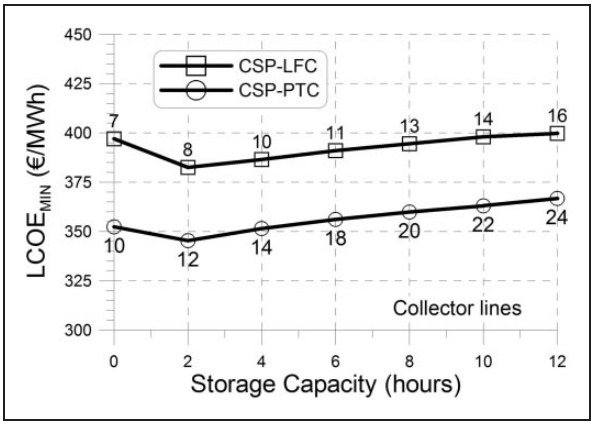

Figure 9. Minimum LCOE of the two CSP power plants in function of storage capacity.

Figure 8 also demonstrates that CSP plants based on PTC give better economic performance than solutions based on LFC (the lowest LCOE is about 340–360 €/MWh for CSP-PTC plants and about 380–400 €/MWh for CSP-LFC ones) mainly due to the higher conversion efficiency of the solar field and therefore to the higher electrical energy production. Similar to Figure 7, Figure 8 demonstrates the importance of a proper trade-off between the main design parameters since for each storage capacity, the LCOE reaches its lowest value for a proper value of the solar multiple.

Figure 9 gives the lowest LCOE for both CSP-PTC and CSP-LFC solutions in function of the storage capacity while plot labels also give the corresponding number of collector rows (the resulting value of the solar multiple can be deduced from Figure 5). In particular, the lowest LCOE for the CSP-PTC plant (340 €/MWh) is achieved with a storage capacity of about 2 h and 12 collector rows (the corresponding solar multiple is about 1.4) while that for the CSP-LFC solution (380 €/MWh) is achieved for the same storage capacity and 8 collector rows (the solar multiple is about 1.6). Obviously, it should be observed that higher energy productions and lower LCOE can be achieved with reference to sites with higher DNI availabilities. For example, the site of Daggett (California, USA), often used as a reference site, is characterized by an annual DNI availability of about 2724 kWh/m^2, which is about 58% higher than that of Cagliari. Therefore, the annual electrical production of a CSP plant located in Daggett is about 50–60% higher than that of the same plant located in Cagliari.

With reference to the cost of the solar field assumed here (200 €/m^2 for LFC and 275 €/m^2 for PTC), the results of the preliminary economic analysis indicate that LFCs are still not competitive with parabolic troughs. A sensitivity analysis to evaluate the LCOE in function of the specific cost of the solar field shows that CSP-LFC solutions could reach the same LCOE of CSP-PTC solutions if their specific costs decrease to about 150–160 €/m^2. This result agrees well with those achieved by similar comparative studies of CSP plants based on parabolic troughs and LFCs, even though the latter studies refer to large-size power plants.[22–24]

The results of this study also demonstrate that the LCOE of 1 MWe CSP plants is significantly higher than those of large-size CSP plants and of nuclear and fossil-fired power plants. For example, the US Department of Energy estimates that the current LCOE for large-size (100–250 MWe) CSP plants based on PTC and thermal oil as heat transfer fluid is about 190–200 $/MWh (about 130–140 €/MWh), with a target of 60–100 $/MWh (45–70 €/MWh) for a 2020 scenario.[31] With reference to nuclear and fossil-fired power plants, the projected costs of generating electricity of the International Energy Agency show that the median values of the LCOE in OECD countries is about 42 €/MWh for nuclear, 61 €/MWh for combined cycles, and 47 €/MWh for coal.[30] Therefore, the achievement of economic competitiveness of CSP plants requires a significant technological development to reduce their capital cost and improve conversion efficiency, especially for medium-size solutions. The development of CSP technology can greatly benefit from the economic grants provided by many national regulations. For example, the Italian regulation for CSP plants connected in the period 2012–2015 offers a feed-in tariff of about 320 €/MWh which is granted for 25 years and which is in addition to the revenues resulting from the sale of electricity on the market.[32] Since the current average prices of electricity range from 60 to 80 €/MWh, the overall revenues for a CSP plant in Italy can be evaluated in the range of 380–400 €/MWh and therefore higher than the LCOE evaluated herein.

Conclusions

In this paper, a comparative performance and cost analysis of medium-size (1 MWe) CSP plants based on an ORC power generation unit integrated with parabolic troughs and LFCs is presented. Owing to the lower land requirement, this kind of CSP plant may be a very interesting option in countries where the areas required by large-size CSP plants are very hard to find.

Annual energy production of the two CSP configurations increases with solar multiple and storage capacity, and for given values of both solar multiple and storage capacity, the use of parabolic trough collectors makes it possible to achieve higher energy yields in comparison to LFCs owing to their better optical efficiency. For example, with a solar multiple equal to 2.0, the CSP-PTC plant produces 20–30% more energy than the CSP-LFC one. The advantage of the CSP-PTC solution decreases to about 15–20% for a SM of about 4.

The results of the performance assessment demonstrate that if land availability is the most limiting factor, CSP solutions based on LFCs could be preferred owing to their higher energy production per m^2

of occupied land (about 50–60 kWh/y per m^2 of occupied land vs. 45–55 kWh/y produced by solutions based on parabolic troughs). However, owing to their better optical efficiency, the use of parabolic troughs gives better values of energy production per unit area of solar collector (about 185–205 kWh/m^2 vs. 125–140 kWh/m^2) and therefore better conversion efficiencies (about 10.8–11.9% vs. 7.3–8.1%).

The results of a preliminary economic analysis shows that the lowest LCOE for the CSP-PTC plant (340 €/MWh) is achieved with a storage capacity of about 2 h and a solar multiple of about 1.4, while that for the CSP-LFC solution (380 €/MWh) is achieved for the same storage capacity and a solar multiple of about 1.6. Therefore, LFCs are still not competitive with parabolic troughs since to achieve the same LCOE the specific cost of LFCs must decrease by about 20–25%. Moreover, the LCOE of medium-size CSP plants is significantly higher than those of large-size CSP plants, nuclear and fossil-fired power plants, and also of PV plants (in the range of 80–120 €/kWh, according to solar energy availability, and the achievement of economic competitiveness of CSP plants requires a significant technological development to reduce their capital cost and to improve their conversion efficiency, especially for medium-size solutions.

Acknowledgements

This work was carried out as part of a collaboration agreement with the "Sardegna Ricerche" Consortium for the management, scientific coordination and development of research activities of the "Concentrated Solar Technologies and Hydrogen from RES Laboratory".

Funding

This research received no specific grant from any funding agency in the public, commercial, or not-for-profit sectors.

Conflict of interest

None declared.

References

1. International Energy Agency, PVPS Report. A Snapshot of Global PV 1992–2012, Report IEA-PVPS T1-22:2013, www.iea-pvps.org.
2. http://www.solarpaces.org (accessed April 2015).
3. http://www.estelasolar.eu (accessed April 2015).
4. Reddy VS, Kaushik SC, Ranjan KR, et al. State-of-the-art of solar thermal power plants – A review. *Renew Sustain Energy Rev* 2012; 27: 258–273.
5. Tian Y and Zhao CY. A review of solar collectors and thermal energy storage in solar thermal applications. *Appl Energy* 2013; 104: 538–553.
6. Kuravi S, Trahan J, Goswami DY, et al. Thermal energy storage technologies and systems for concentrating solar power plants. *Prog Energy Combust Sci* 2013; 39: 285–319.
7. Zhang HL, Baeyens J, Degrève J, et al. Concentrated solar power plants: Review and design methodology. *Renew Sustain Energy Rev* 2013; 22: 466–481.
8. Fernández-García A, Zarza E, Valenzuela L, et al. Parabolic-trough solar collectors and their applications. *Renew Sustain Energy Rev* 2010; 14: 1695–1721.
9. Kearney D, Kelly B, Herrmann U, et al. Engineering aspects of a molten salt heat transfer fluid in a trough solar field. *Energy* 2004; 29: 861–870.
10. Zaversky F, Medina R, García-Barberena J, et al. Object-oriented modeling for the transient performance simulation of parabolic trough collectors using molten salt as heat transfer fluid. *Sol Energy* 2013; 95: 192–215.
11. Feldhoff JF, Schmitz K, Eck M, et al. Comparative system analysis of direct steam generation and synthetic oil parabolic trough power plants with integrated thermal storage. *Sol Energy* 2012; 86: 520–530.
12. Zarza E, Rojas ME, González L, et al. INDITEP: The first pre-commercial DSG solar power plant. *Sol Energy* 2006; 80: 1270–1276.
13. Ramos A and Ramos F. Strategies in tower solar plant optimization. *Sol Energy* 2012; 86: 2536–2548.
14. Collado FJ and Gullar J. A review of optimized design layouts for solar power tower plants with campo code. *Renew Sustain Energy Rev* 2013; 20: 142–154.
15. Bakos GC and Parsa D. Technoeconomic assessment of an integrated solar combined cycle power plant in Greece using line-focus parabolic trough collectors. *Renew Energy* 2013; 60: 598–603.
16. Cau G, Cocco D and Tola V. Performance and cost assessment of integrated solar combined cycle systems (ISCCSs) using CO_2 as heat transfer fluid. *Sol Energy* 2012; 86: 2975–2985.
17. Peterseim HJ, White S, Tadros A, et al. Concentrated solar power hybrid plants, which technologies are best suited for hybridisation? *Renew Energy* 2013; 57: 520–532.
18. Al-Sulaiman FA, Hamdullahpur F and Dincer I. Performance assessment of a novel system using parabolic trough solar collectors for combined cooling, heating, and power production. *Renew Energy* 2012; 48: 161–172.
19. Tchanche BF, Lambrinos G, Frangoudakis A, et al. Low-grade heat conversion into power using organic Rankine cycles - A review of various applications. *Renew Sustain Energy Rev* 2011; 15: 3963–3979.
20. Vélez F, Segovia JJ, Martín MC, et al. A technical, economic and market review of organic Rankine cycles for the conversion of low-grade heat for power generation. *Renew Sustain Energy Rev* 2012; 16: 4175–4189.
21. Giostri A, Binotti M, Silva P, et al. Comparison of two linear collectors in solar thermal plants: Parabolic trough versus Fresnel. *J Solar Energy Eng* 2013; 135: paper number 11001.
22. Zhu G, Wendelin T, Wagner MJ, et al. History, current state, and future of linear Fresnel concentrating solar collectors. *Sol Energy* 2014; 103: 639–652.
23. Morin G, Dersch J, Platzer W, et al. Comparison of linear Fresnel and parabolic trough collector power plants. *Sol Energy* 2012; 86: 1–12.
24. Schenki H, Hirsch T, Feldhoff JF, et al. Energetic comparison of linear Fresnel and parabolic trough collector systems. In: *Proceedings of the ASME 2012 6th international conference on energy sustainability*, ES2012, 23–26 July 2012, San Diego, CA, USA, Paper number ES2012-91109.

25. Gil A, Medrano M, Martorell I, et al. State of the art on high temperature thermal energy storage for power generation. Part 1—Concepts, materials and modellization. *Renew Sustain Energy Rev* 2010; 14: 31–55.
26. Wagner SJ and Rubin ES. Economic implications of thermal energy storage for concentrated solar thermal power. *Renew Energy* 2014; 61: 81–95.
27. Meteonorm, Version 6.0, Meteotest, Bern (CH), 2010.
28. NREL, SAM Linear Fresnel Model Reference Manual, www.sam.nrel.gov (accessed April 2014).
29. http://www.turboden.eu (accessed April 2014).
30. International Energy Agency (IEA) and OECD Nuclear Energy Agency (NEA), Projected costs of generating Electricity – 2010 Edition, Report IEA-NEA, ISBN 978-92-64-08430, www.iea.org.
31. US Department of Energy, SunShot Vision Study, February 2012, www1.eere.energy.gov.
32. Gestore dei Servizi Energetici (GSE), Solar thermodynamic Feed-in scheme, www.gse.it/en/feedintariff (accessed April 2014).

Appendix

Notation

A_C	collecting area
$C_{O\&M,k}$	operation and maintenance cost in year "k"
E_k	electricity production in year "k"
F	focal length
I_k	investment cost in year "k"
i	annual interest ratio
L	collector length
m	mass
N	operating life time
R	rows distance
Q	thermal power
T	temperature
W	collector width
V	volume
α	elevation angle
η	efficiency
γ	azimuth angle
θ	incidence angle